Research Article GU J Sci, Part A, 11(1): 225-234 (2024) 10.54287/gujsa.1433100

Gazi University
Journal of Science
PART A: ENGINEERING AND INNOVATION
http://dergipark.org.tr/gujsa

Study on the Optical and Gas-Sensing Performance of Zn-doped CuO Films

Sezen TEKIN[1*]

[1] *Department of Medical Services and Techniques, Eldivan Medical Services Vocational School, Çankırı Karatekin University, Çankırı, Türkiye*

Keywords

CuO Thin Films
Linear Optics
Gas-Sensing
Dopant Effect

Abstract

The pure copper oxide thin film was deposited on glass substrates by SILAR method with 30 cycles. To examine the doping effect, Zn-doped films at different doping ratios were prepared under the same conditions as the undoped film. The XRD, SEM and Raman measurements were performed to investigate the morphological and structural properties of the samples. Analysis showed increasing aggregation and amorphous structure with doping. The optical parameters were characterized by spectrophotometer measurement and relevant formulas. The band gap energies were determined to increase from 2.50 to 2.79 eV with the increasing Zn rate. The Hervé and Vandamme, Moss and Ravindra relations were used to determine the refractive index. The room temperature gas-sensing performance for the undoped and doped samples were reported and the responses for 5 ppm gas were calculated as 249 %, 800 %, 189 % and 15 % for the CuO, 1Zn:CuO, 3Zn:CuO and 5Zn:CuO, respectively. The response of CuO thin films changed with doping, and 1% Zn doping rate was determined as the optimal rate in this study.

Cite

Tekin, S. (2024). Study on the Optical and Gas-Sensing Performance of Zn-doped CuO Films. *GU J Sci, Part A*, *11*(1), 225-234. doi:10.54287/gujsa.1433100

Author ID (ORCID Number)

0000-0002-6599-9631 Sezen TEKIN

Article Process

Submission Date 07.02.2024
Revision Date 20.02.2024
Accepted Date 06.03.2024
Published Date 22.03.2024

1. INTRODUCTION

CuO is a p-type semiconductor, and one of the transition metal oxides (TMOs) with a relatively small monoclinic crystal system. CuO films are used in numerous application areas such as photocatalysts, gas sensors, solar cells, field emission devices, high temperature superconductors and lithium batteries, due to the advantages of copper being abundant in nature, having a low production cost, being non-poisonous, and having high thermal stability, optical and electrical properties (Mnethu et al., 2020). Metal doping, the addition of the impurity ions to its lattice, is one of the known methods to control the properties of a semiconductor. The transition metals and rare-earth metals can be as doping materials. Various thin film preparation methods are available in the literature, but among them, the SILAR method is one of the simplest and most cost-effective techniques as it is flexible in the selection of substrates, at low processing temperatures, repeatable and provides large-area production (Mnethu et al., 2020).

There are some reports based on optical properties, gas selectivity and sensitivity for undoped and doped CuO produced by different methods. For example, Mnethu et al. (2020) deposited CuO and Zn doped CuO nanoplatelets by hydrothermal synthesis and investigate the sensing characteristics at various concentrations and for 9 different gases. In another study, the temperature dependent conductivity and energy band structure of p-type amorphous film produced by magnetron sputtering method were investigated with the theoretical calculation and experimental measurement (Huang et al., 2015). Maebana et al. (2023) reported extremely sensitive and selective xylene detector system produced from CuO-ZnO. Ezenwa (2012) studied optical and structural characterization of the films with 1.7 eV and high density of grains, deposited on glass with chemical

*Corresponding Author, e-mail: sezentekin@karatekin.edu.tr

bath deposition at 300K. The variation of refractive index and other optical properties with PEG content were investigated by Çavuşoğlu (2018). The optical band gap energies increased, and film thickness reduced depending on the increasing amount of PEG (Çavuşoğlu, 2018).

The aim of this study is to control the optical and gas sensing properties of pure CuO films, deposited with SILAR method using Zn doping and doping ratio variation under constant production conditions.

2. MATERIAL AND METHOD

The undoped and Zn-doped CuO thin films were produced by SILAR with 30 cycles.The SILAR cycle was performed as follows: The glass substrate was kept in CuO solution for 20 sec. Then the substrate was removed from the solution and immediately immersed in hot water at 90℃ for 7 sec. After hot water, the substrate was left in the air for 1 minute, and then the cycle was completed by dipping it into deionized water for 30 sec. In this way, the undoped CuO thin film were grown on the glass substrate in 30 cycles, and the same cycle was performed for Zn-doped CuO solution. To see the effect of the doping rate, the Zn ratio in the solution was changed as 0, 1, 3 and 5%. and the films were coded as CuO, 1Zn:CuO, 3Zn:CuO and 5Zn:CuO, respectively. The structural properties of the CuO and (M) Zn:CuO (M=1,3,5) films were researched using XRD, SEM and Raman spectroscopy. The linear absorbance of all produced films were measured with SHIMADZU double beam spectrophotometer (model UV-1800) in a wavelength range of 300–1000 nm. The produced sensors will be tested electrically, and 99.999% purity CO_2 gas will be used in these testing stages. Since the measurements had to be carried out in a CO_2 atmosphere for the sensor tests, a sealed chamber and probe tips positioned inside the chamber were used. Gas sensor measurement system consists of Keithley 2400, LakeShore 325 temperature controller, Keysight E4990A impedance meter, MKS flow controllers (MFC), modified sensor cell for gas measurements, dry air, CO_2 gas and vacuum pump. Gas sensor cell; It consists of a sample holder, gas valves that provide the inlet and outlet of the target gas, and BNC connectors for connecting the sensor to the Keithley 2400 device and the Keysight E4990A impedance device. Gas flow was provided by the mass flow controller (MFC) and the measuring chamber outlet was connected to the exhaust line. By measuring the base resistance of the sensors in the atmospheric environment, the resistance change that occurred after the start of CO_2 gas flow was examined. The obtained measurement data were instantly transferred to the computer and recorded.

3. RESULTS AND DISCUSSION

The SEM images of the produced (a) CuO, (b) 1Zn:CuO, (c) 3Zn:CuO and (d) 5Zn:CuO are represented in Figure 1. The produced CuO sample is distributed homogeneously on the surface and its size is clearly visible. With the doping, the samples started to clump and the size change of the CuO nanoparticles with the creation of aggregation and small nanostructures was observed.

The XRD patterns of the undoped and Zn-doped films are given in Figure 2. The peaks observed in the produced CuO and 1Zn:CuO films at ~ 35° and 38° specify (-111) and (111) reflections. However, when the XRD analysis of the structures is examined completely, they are seen to be amorphous. No peak was observed for the 3Zn:CuO and 5Zn:CuO samples, indicating that the deposited films had an amorphous structure. This may be related to the growth method. The observed results were associated with the literature results (Patil et al., 2017; Daoudi et al., 2019). Patil et al. (2017) reported that an amorphous structure was observed in the XRD analysis of CuO thin films produced by SILAR method. In the XRD analysis of CuO thin films obtained by Daoudi et al. (2019) it was reported that the intensities of the peaks were low and almost amorphous structures grew.

Raman spectroscopy, one of the important techniques used to examine the vibration properties and structure of the produced films, is given in Figure 3. The peaks seen between 557-554 and 784-786 cm^{-1} and shown in yellow are associated with ZnO and indicate the presence of dopant atoms in the structure. While A_g mode was obtained as 278, 276, 275 and 273 cm^{-1}, $B_{g(1)}$ mode was found as 330, 328, 327 and 325 cm^{-1} for CuO, 1Zn:CuO, 3Zn:CuO and 5Zn:CuO, respectively. And also, 613, 609 and 607 cm^{-1} were observed for $B_{g(2)}$ mode. When the dopant atoms were included into the structure, a blue shift for the A_g, $B_{g(1)}$ and $B_{g(2)}$ modes was obtained.

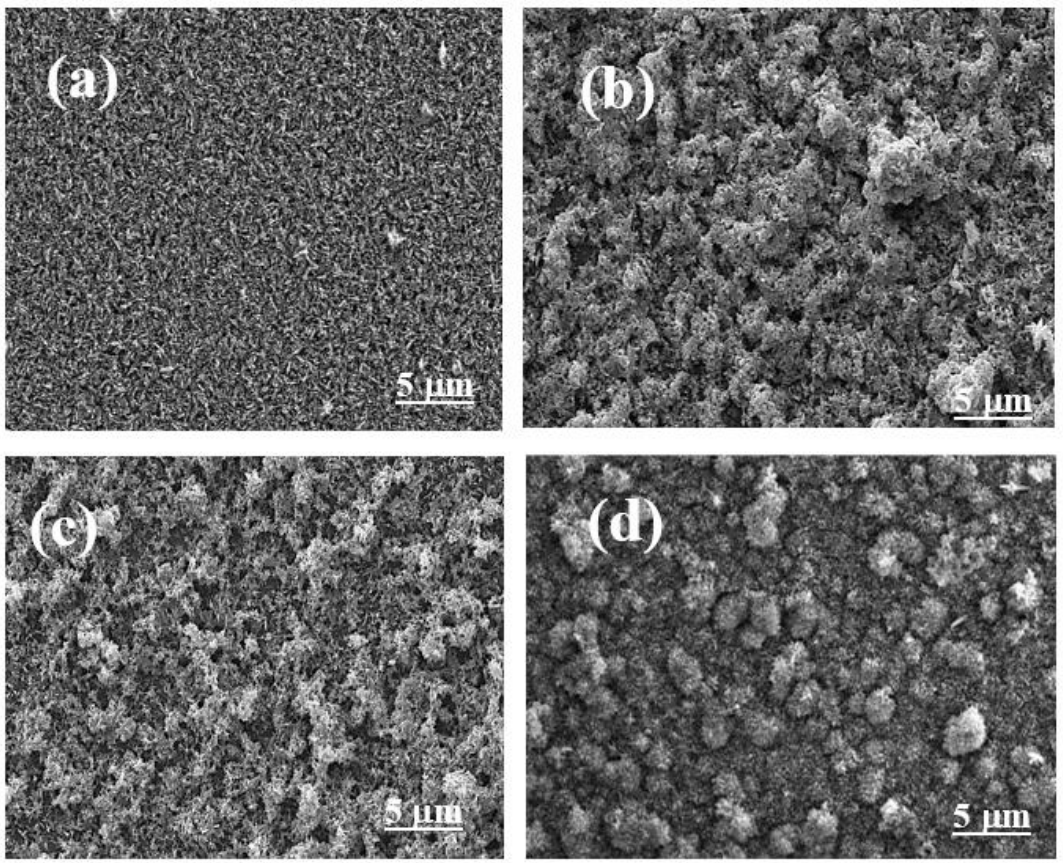

Figure 1. *The SEM analysis of produced films*

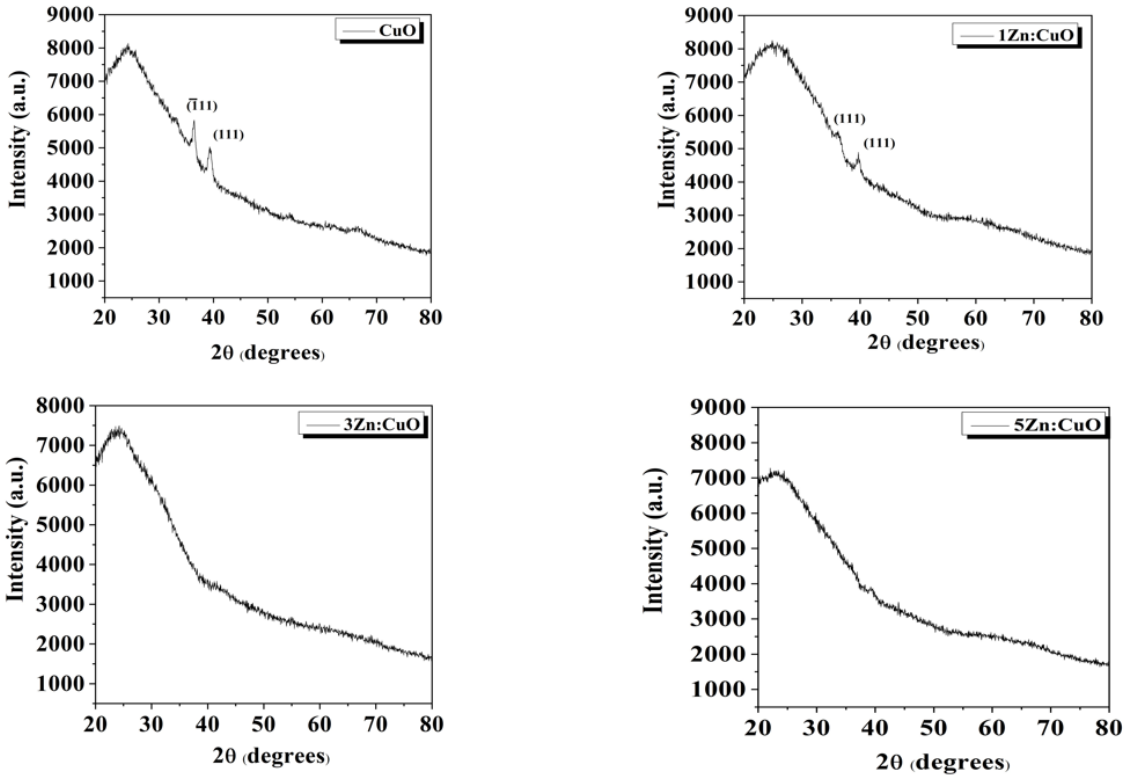

Figure 2. *The XRD for the produced samples*

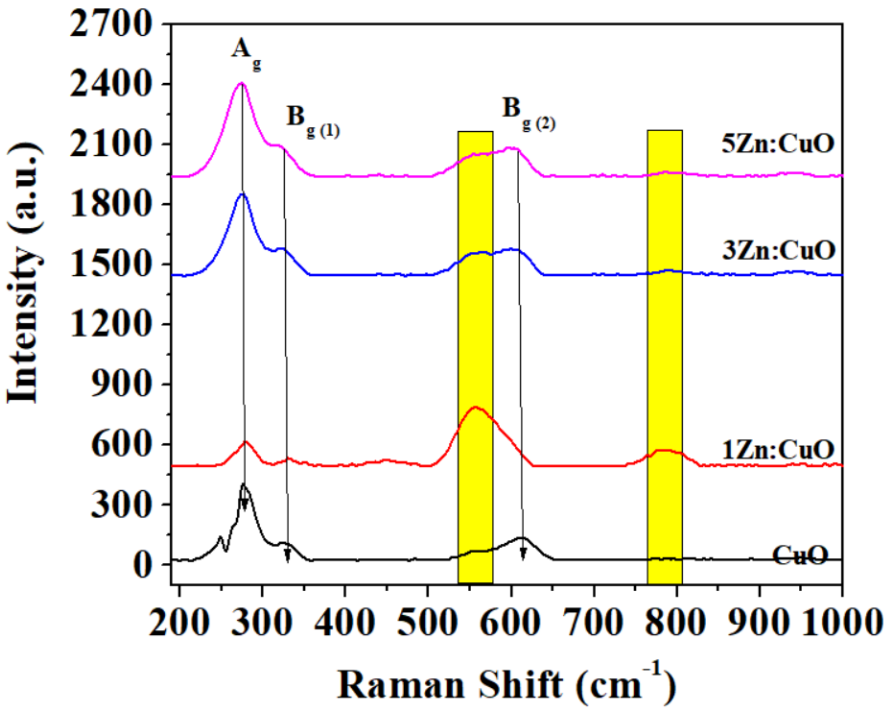

Figure 3. *The Raman spectra of produced films*

Figure 4 depicts the linear absorption of the CuO and (M) Zn:CuO (M=1,3,5) films. The absorption decreased towards longer wavelengths for all samples. As seen from the figure, as the Zn additives ratio increases, the absorbance feature decreases. The absorption (α) and extinction (k) coefficient are defined using absorption results and related by $\alpha=2.303A/d$ and $k=\alpha\lambda/4\pi$ (Dhineshbabu et al., 2016). The α (Figure 5) and k (Figure 6) coefficient results are compatible with the absorption graph (Figure 4) as expected. It is clear from Figure 5 that the high values of α ($> 10^4$ cm^{-1}) are obtained for all films, so, the direct transition can be mentioned. This result agrees with literature (Balamurugan & Mehta, 2001; Ezenwa, 2012).

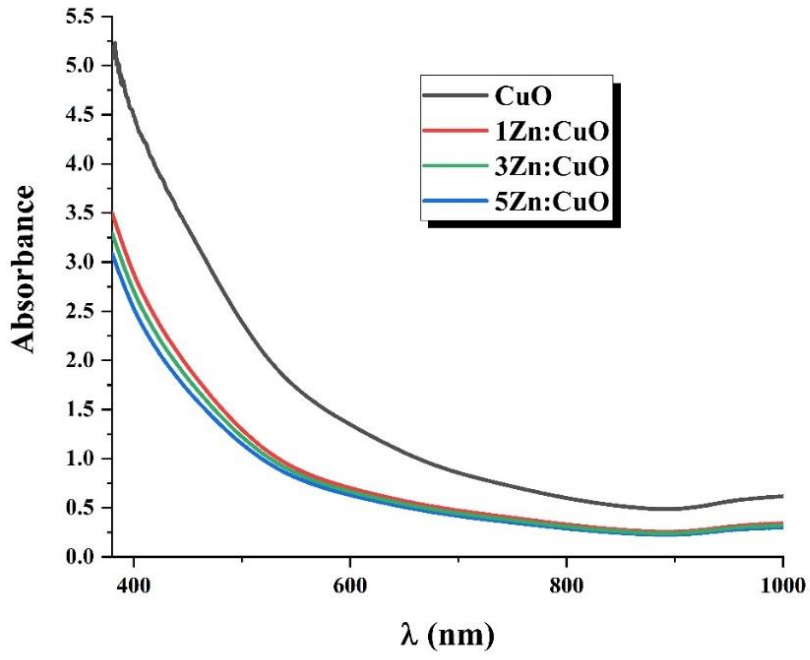

Figure 4. *The absorbance vs. wavelength for undoped and doped samples*

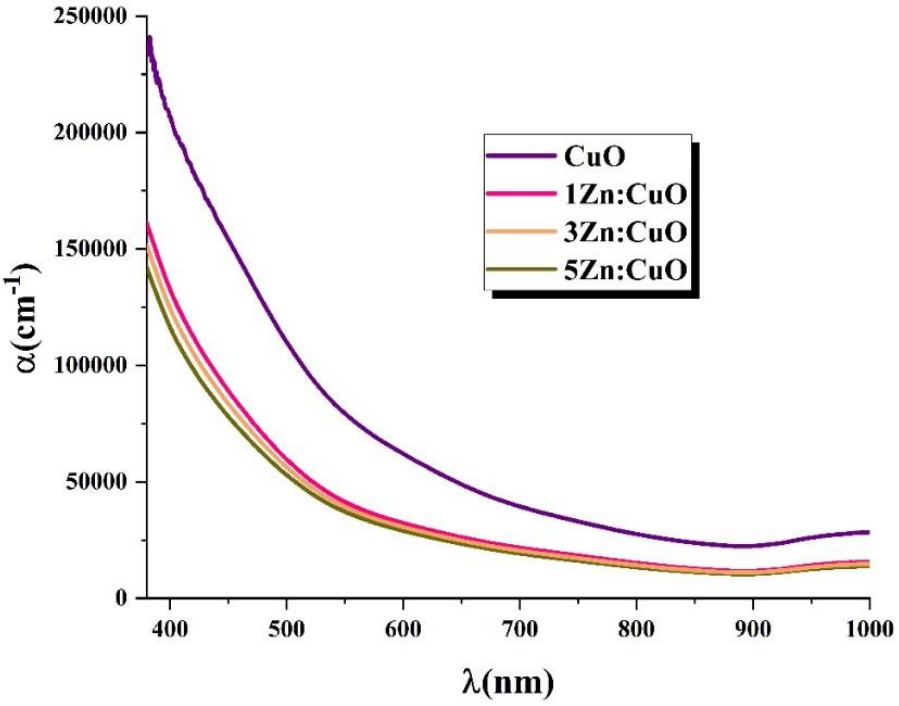

Figure 5. *The α vs. wavelength of the produced films*

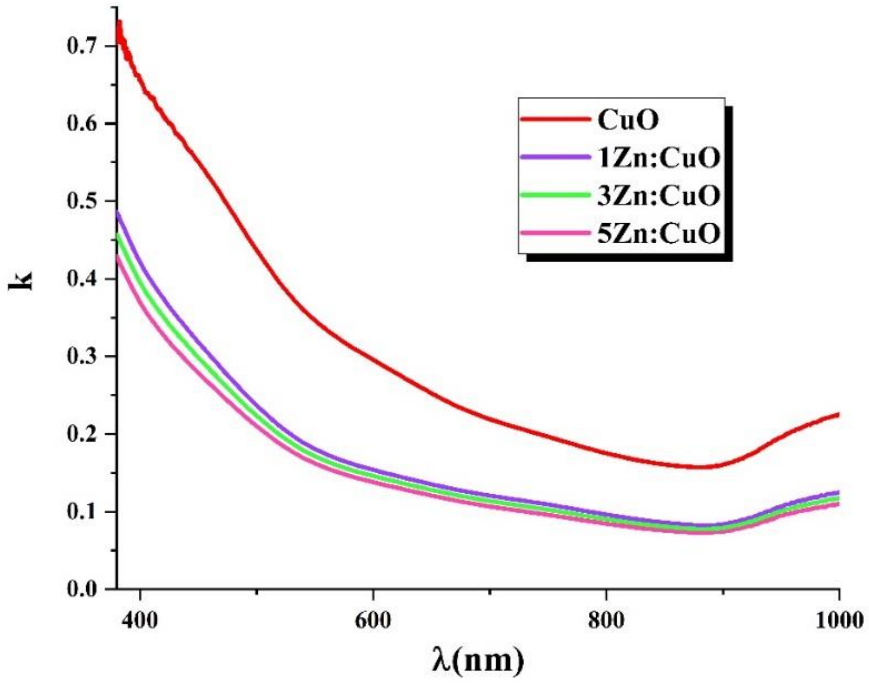

Figure 6. *The extinction coefficient for all films*

Figure 7 depicts a plot of $(\alpha h\upsilon)^2$ vs. photon energy to find the band gap for CuO and (M) Zn:CuO (M=1,3,5) samples. Eg energy ranges were determined at the point where the linear part of these graphs intersects the energy axis at $(\alpha h\upsilon)^2=0$. As seen in Table 1, the band gaps are defined as 2.50, 2.69, 2.75 and 2.79 eV for CuO, 1Zn:CuO, 3Zn:CuO and 5Zn:CuO, respectively. CuO has a relatively low bandgap (1.2-1.9 eV) (Lu et al., 2009). The pure CuO film in our study has a higher band gap, and this can be explained by the amorphous structure (Figure 2) and aggregation (Figure 1). There are other studies in the literature that achieve high bandgap such as 2.24 (Güngör, 2019) and 3,19 eV (Das & Alford, 2013). The band gap values of the films increase depending on the increasing Zn concentration; as shown in Figure 7. This change in optical band gap energy values is a result of the change in the amorphous structure of Zn:CuO films (Figure 2) with increasing amounts of Zn doping. Huang et al. (2015) reported the similar behavior for crystalline and amorphous Cu_2O films. They obtained ~2.0 and ~2.7 eV for the crystalline and amorphous films, respectively. Additionally, Abdel Rafea and Roushdy (2009) reported a decreasing band gap from 2.3 to 1.7 eV due to annealing and crystallization.

The refractive index (n) of the films can be determined with different models. The Hervé and Vandamme (Hervé & Vandamme, 1994), Moss and Ravindra (Tripathy, 2015) relations were used, and the results are given in Table 1. The value of the refractive index is compatible with Ezenwa (2012) which found it as 2.7 for CuO thin films. Çavuşoğlu (2018) determined higher refractive index values (~3.02, ~3.06) using the Moss and Hervé and Vandamme model. This is due to the lower band gap of the films in the study.

Table 1. *Optical calculations for all films*

Samples	**E_g** (eV)	**n** (Moss)	**n** (Ravindra)	**n** (Hervé & Vandamme)
CuO	2.50	2.48	2.53	2.51
1Zn:CuO	2.69	2.44	2.42	2.45
3Zn:CuO	2.75	2.42	2.38	2.43
5Zn:CuO	2.79	2.41	2.35	2.41

Gas sensors often indicate the presence of a toxic gas in room conditions. Therefore, under normal room conditions, in the presence of only air, the parameter to be measured must be constant. For this purpose, the change over time of the current parameter used in the study was measured. Dynamic CO_2 gas sensor measurements were performed at room temperature in the air environment (Figure 8). First, dry air was sent at a constant flow rate to ensure that the surface was stable. Then, different concentrations of CO_2 gas were sent. The experimental results showed that the sensors of different designs covering the same area, under the same gas flow, operate with lower sensitivity as the additive ratio increases (except 1Zn:CuO). It was observed that the 5Zn:CuO sensor reached its saturation point and was not sensitive to different gas concentrations.

Since CuO is a p-type and ZnO is an n-type semiconductor, a p-n heterojunction structure is formed by doping Zn into the CuO structure. As a result of this joint structure, an increase in current conduction is observed (Poloju et al., 2018). The hole density in the p-type semiconductor and the electron density in the n-type semiconductor are high, and the Fermi energy levels also differ from each other. Therefore, when these two structures are brought atomically close to each other, a flow of electrons occurs between them. It causes a bending of the energy band structures associated with p- and n-type semiconductors when they are combined. For this reason, an increase is observed in doped thin films compared to the response of undoped CuO thin films. However, there was a decrease after a certain doping rate and 1% doping rate was determined as the optimal doping rate in this study. Maebana et al. (2023) have reported the gas sensing properties of the Zn-doped CuO structure and observed that there was a decrease in sensitivity with increasing Zn doping. The highest response was obtained for 1 % Zn-doped CuO. They attributed this to aggregation between ZnO and CuO , thus reporting a lower detection performance (Maebana et al., 2023). Mnethu et al. (2020) have determined the selective behavior with responses of 42 and 53 for pure CuO and 0.1% doped Zn:CuO, respectively. They commented that the hypothesized mechanism of electronic chemo-resistant gas sensing goes beyond the attributes of intrinsic defects such as oxygen vacancies and their interstitials.

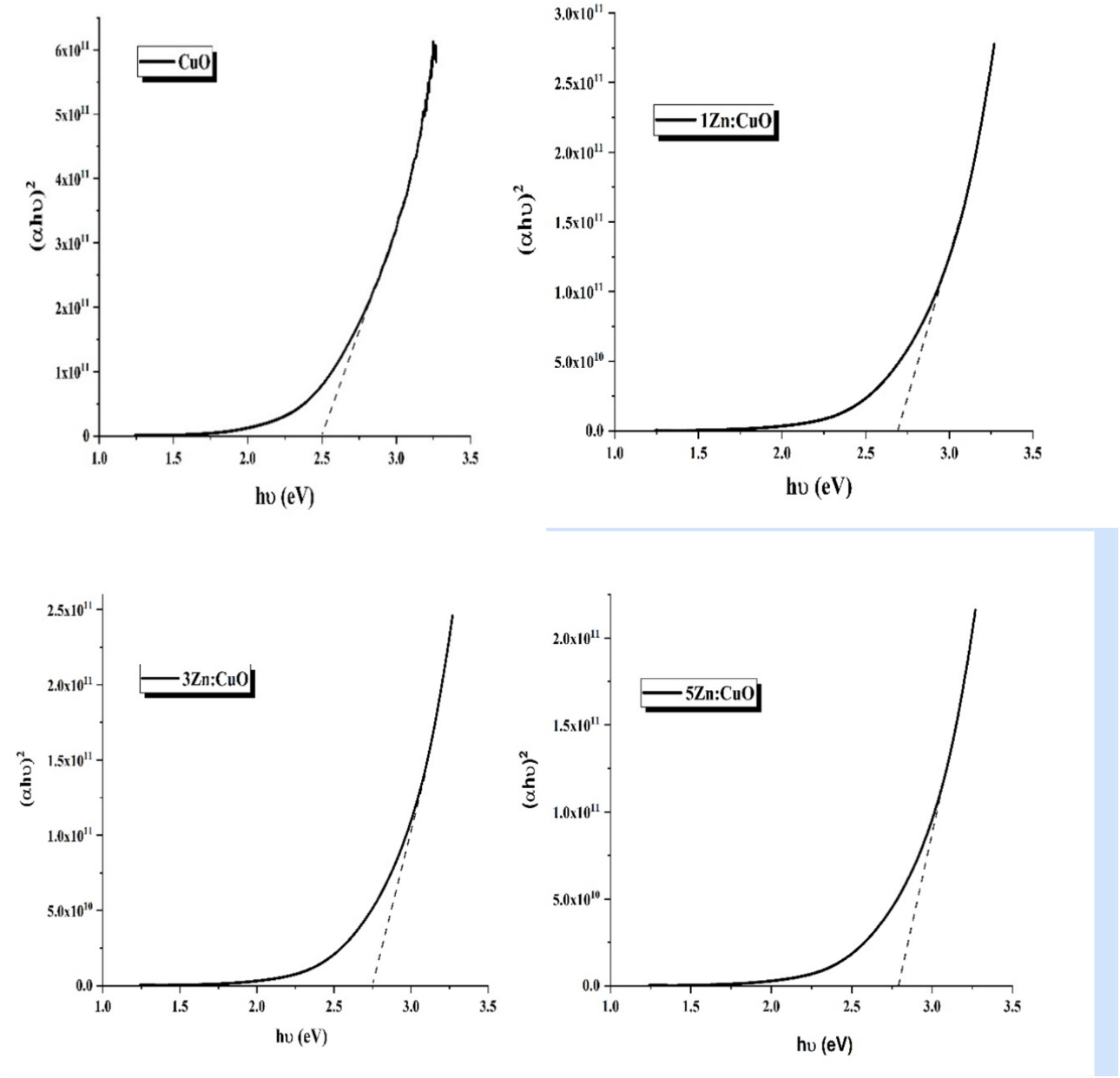

Figure 7. *Tauc plots for undoped and doped samples*

Figure 9 depicts the responses vs. gas concentrations for the produced samples. The responses of the 5 ppm CO_2 gas were calculated 249 %, 800 %, 189 % and 15 % for the CuO, 1Zn:CuO, 3Zn:CuO and 5Zn:CuO, respectively. No selectivity was observed for the 5Zn:CuO sample towards different gas concentrations, although a small amount of sensitivity was obtained when the gas was sent to the surface. The maximum sensitivity was obtained for the 1Zn:CuO sample. When the 3Zn:CuO sample was examined, a decrease in sensitivities began to be seen. The results obtained are compatible with the literature (Mnethu et al., 2020; Maebana et al., 2023). Differences in responses were observed depending on the doping rate, and the responses started to decrease after 1% Zn. Therefore, to achieve an increase in sensitivity, lower additive rates should be preferred. At higher Zn concentrations, neutral defects gradually form, which causes the charge carriers to be neutralized between the p-n heterojunction (Yathisha & Arthoba, 2018). As seen in Figure 9, the lowest sensitivity was obtained at 1 ppm for all samples. The responses of the 1 ppm CO_2 gas were calculated 136%, 201 %, 50 % and 15 % for the CuO, 1Zn: CuO, 3Zn:CuO and 5Zn:CuO, respectively. Response and recovery times of the produced samples are represented in Figure 10. Since no selectivity towards gases was observed

for the 5Zn:CuO sample, response and return calculations were not made and the graph included only 3 samples. The response and recovery times at room temperature (1 ppm) were calculated 1.7, 1.5, 1.5 minutes and 0.7, 0.6 and 0.6 minutes for the CuO, 1Zn: CuO and 3Zn:CuO, respectively; as shown in Figure 10. It is important that the produced sensor materials have low response and return times to be used commercially. Sensor devices produced from materials with fast response and return times for application areas such as mining are of great importance in protecting human health.

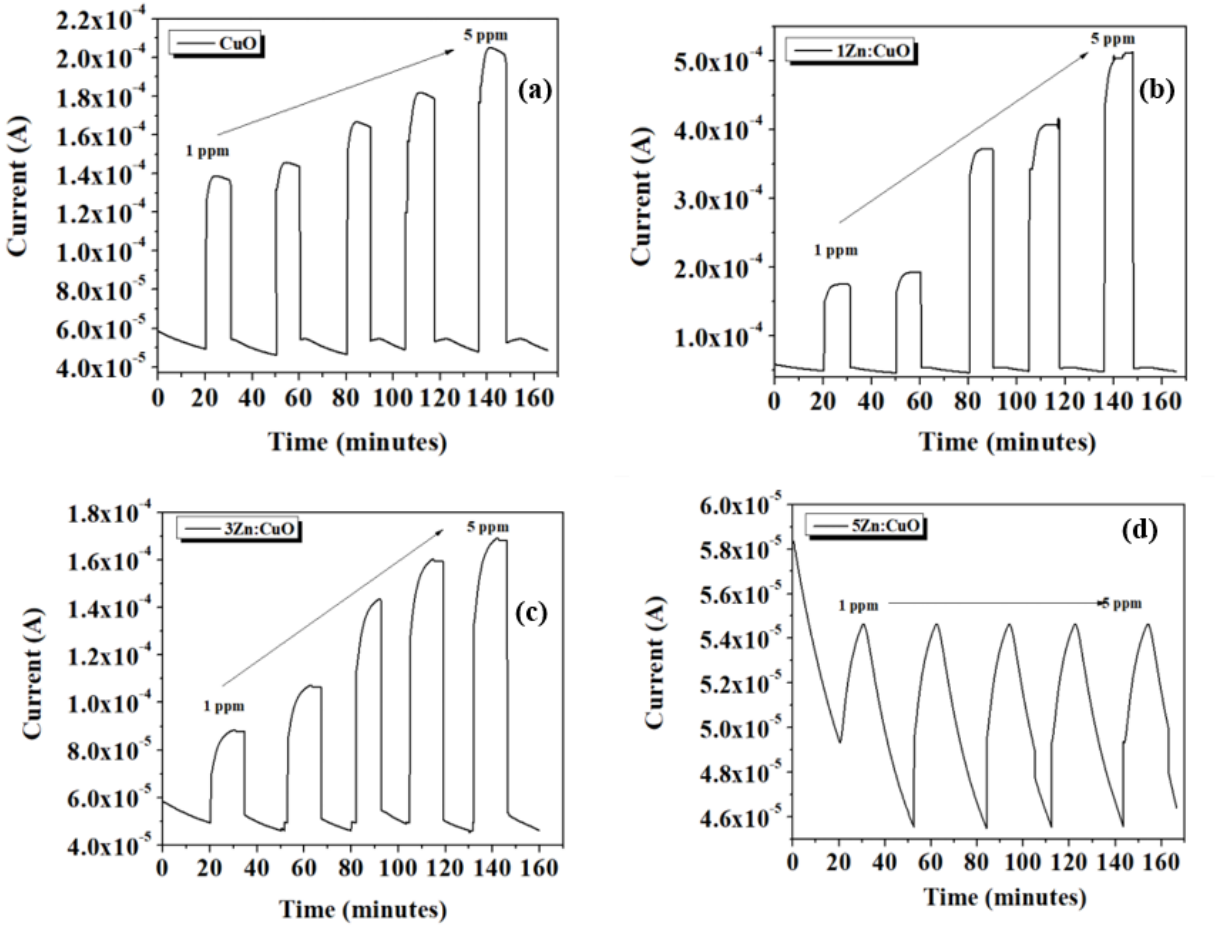

Figure 8*. The dynamic gas sensing measurements of the produced films*

4. CONCLUSION

The preparation of undoped and Zn-doped CuO films with different doping ratios have been successfully carried out using SILAR method. When the SEM and XRD analysis of the produced films were examined, increasing aggregation and amorphous structure were observed as the doping rate increased. The doping led to increase the band gap; however, the absorbance was reduced with increasing Zn content. The obtained absorption coefficient values confirmed that there was a direct transition for CuO. Theoretical calculations of the refractive index were made using different models and were compatible with each other and with the literature. Gas sensor measurements were performed at room temperature to investigate the doping effect. It was observed that an increase is occurred for doped thin films compared to the response of undoped CuO thin films. However, there was a decrease after a certain doping rate and 1%Zn doping rate was determined as the optimal rate in this study. The results showed that Zn doping strongly affected the structural, optical, and gas-sensing properties of CuO films. The thin films examined in this study may have potential applications in the optics and sensor industries.

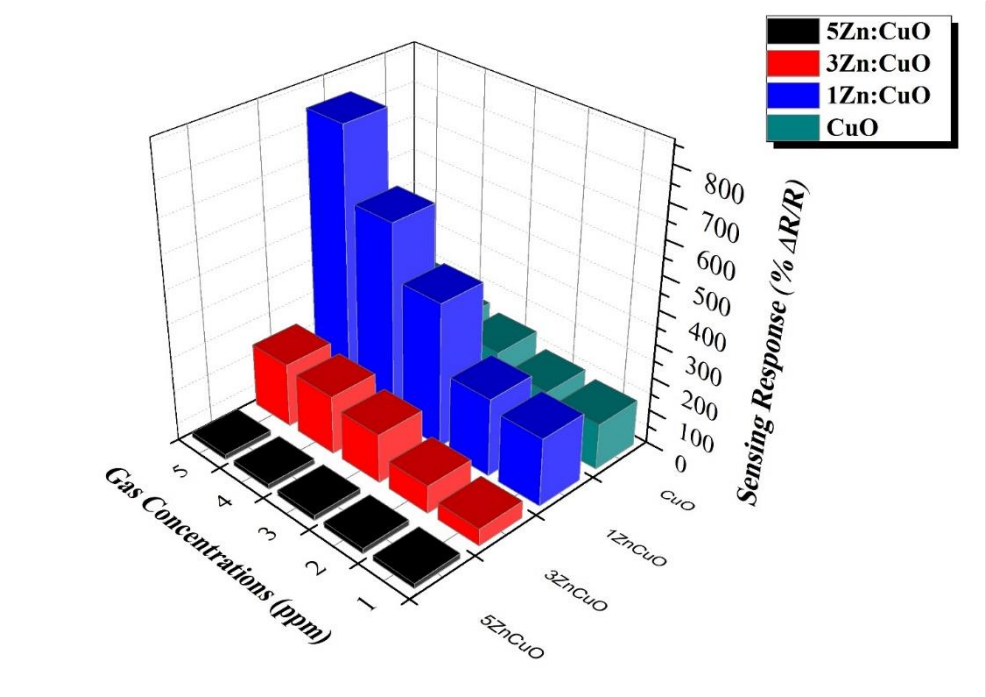

Figure 9. *Response of the produced samples versus gas concentrations*

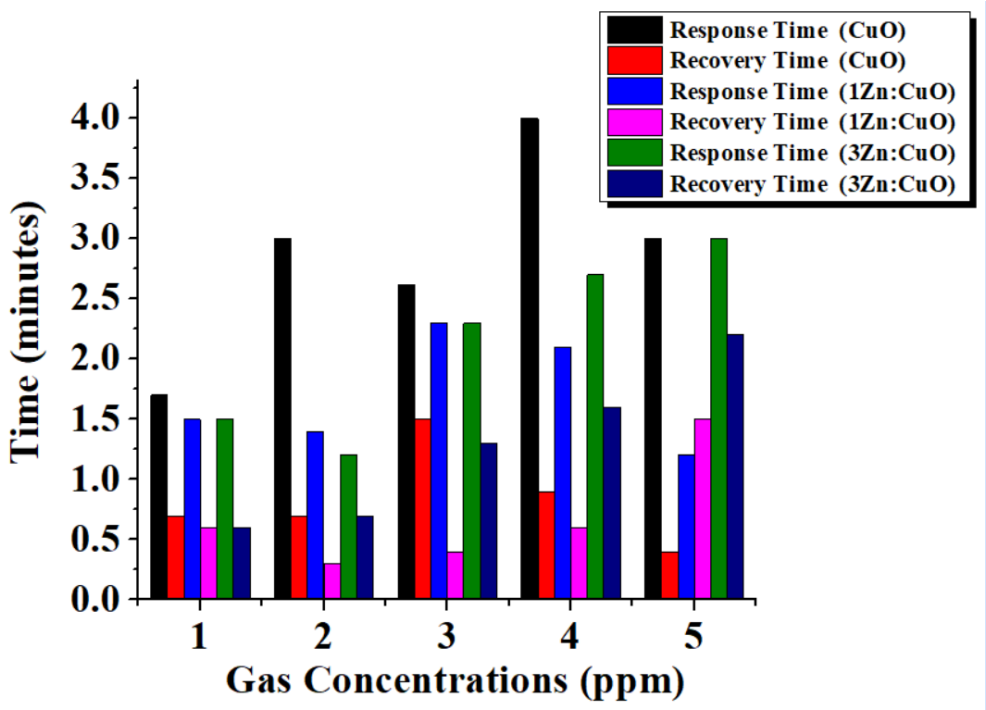

Figure 10*. Response and recovery times of the produced samples*

CONFLICT OF INTEREST

The author declares no conflict of interest.

REFERENCES

Abdel Rafea, M., & Roushdy, N. (2009). Determination of the optical band gap for amorphous and nanocrystalline copper oxide thin films prepared by SILAR technique. *Journal of Physics D: Applied Physics*, *42*, 015413. https://doi.org/10.1088/0022-3727/42/1/015413

Balamurugan, B., & Mehta, B. (2001). Optical and structural properties of nanocrystalline copper oxide thin films prepared by activated reactive evaporation. *Thin Solid Films*, *396*(1-2), 90-96. https://doi.org/10.1016/S0040-6090(01)01216-0

Çavuşoğlu, H. (2018). Band-gap Control of Nanostructured CuO Thin Films using PEG as a Surfactant. *European Journal of Science and Technology*, *13*, 124-128. https://doi.org/10.31590/ejosat.417941

Daoudi, O., Qachaou, Y., Raidou, A., Nouneh, K., Lharch, M., & Fahoume, M. (2019). Study of the physical properties of CuO thin films grown by modified SILAR method for solar cells applications. *Superlattices and Microstructures*, *127*, 93-99. https://doi.org/10.1016/j.spmi.2018.03.006.

Das, S., & Alford, T. L. (2013), Structural and optical properties of Ag-doped copper oxide thin films on polyethylene napthalate substrate prepared by low temperature microwave annealing. *Journal of Applied Physics*, *113*, 244905. https://doi.org/10.1063/1.4812584

Dhineshbabu, N. R., Rajendran, V., Nithyavathy, N., & Vetumperumal, R. (2016) Study of structural and optical properties of cupric oxide nanoparticles. *Applied Nanoscience*, *6*, 933-939. https://doi.org/10.1007/s13204-015-0499-2

Ezenwa, I. (2012). Optical Analysis of Chemical bath Fabricated Cuo Thin Films. *Research Journal of Recent Sciences*, *1*(1), 46-50.

Güngör, E. (2019). Zn:CuO Heteroyapıların Yapısal, Optik, Fotolüminesans ve İletim Özellikleri. *Nevsehir Journal of Science and Technology*, *8*(1), 1-13 https://doi.org/10.17100/nevbiltek.509354

Hervé, P., & Vandamme, L. K. J. (1994). General relation between refractive index and energy gap in semiconductors. *Infrared Physics & Technology*, *35*(4), 609-615. https://doi.org/10.1016/1350-4495(94)90026-4

Huang, Q., Li, J., & Bi, X. (2015). The improvement of hole transport property and optical band gap for amorphous Cu_2O films. *Journal of Alloys and Compounds*, *647*, 585-589. https://doi.org/10.1016/j.jallcom.2015.06.147

Lu, H.-C., Chu, C.-L., Lai, C.-Y., & Wang, Y.-H. (2009). Property Variations of Direct-Current Reactive Magnetron Sputtered Copper Oxide Thin Films Deposited at Different Oxygen Partial Pressures. *Thin Solid Films*, *517*(15), 4408-4412. https://doi.org/10.1016/j.tsf.2009.02.079

Maebana, L. M.., Motsoeneng, R. G., Tshabalala, Z. P., Swart, H. C., Cummings, F. R., Jozela, M., Nkosi, S. S., & Motaung, D. E. (2023). Low-operational temperature for selective detection of xylene gas using a p-n CuO-ZnO heterostructure-based sensor. *Journal of Alloys and Compounds*, *960*, 170683. https://doi.org/10.1016/j.jallcom.2023.170683

Mnethu, O., Nkosi, S. S., Kortidis, I., Motaung, D. E., Kroon, R. E., Swart, H. C., Ntsasa, N. G., Tshilongo, J., & Moyo, T. (2020). Ultra-sensitive and selective p-xylene gas sensor at low operating temperature utilizing Zn doped CuO nanoplatelets: Insignificant vestiges of oxygen vacancies. *Journal of Colloid and Interface Science*, *576*, 364-375, https://doi.org/10.1016/j.jcis.2020.05.030

Patil, A. S., Patil, M. D., Lohar, G. M., Jadhav, S. T., & Fulari, V. J. (2017). Supercapacitive properties of CuO thin films using modified SILAR method. *Ionics*, *23*, 1259-1266 https://doi.org/10.1007/s11581-016-1921-9

Poloju, M., Jayababu, N., & Ramana Reddy, M. V. (2018). Improved gas sensing performance of Al doped ZnO/CuO nanocomposite based ammonia gas sensor. *Materials Science and Engineering: B*, *227*, 61-67. https://doi.org/10.1016/j.mseb.2017.10.012.

Tripathy, S. K. (2015). Refractive indices of semiconductors from energy gaps. *Optical Materials*, *46*, 240-246 https://doi.org/10.1016/j.optmat.2015.04.026

Yathisha, R. O., & Arthoba, N. Y. (2018). Structural, optical and electrical properties of zinc incorporated copper oxide nanoparticles: doping effect of Zn. *Journal of Materials Science*, *53*, 678-691. https://doi.org/10.1007/s10853-017-1496-5